Effect of Heat Treatment Parameters on Microstructure and Mechanical Properties of (AISI1005) Steel

Hassanen L. Jaber, R. K. Salim, Ashraf s. fahad

Abstract

This study aims to investigate tensile properties and work hardening behavior of dual phase (DP) steels. A series of DP steels containing ferrite and martensite with different volume fractions of martensite (*V*m) were produced by intercritical heat treatment. Microstructural investigations, hardness test, and tensile test were carried out. The experimental results showed that dual phase steels at 760^{o}c and 10s have excellent mechanical properties in terms of tensile strength, ductility and fracture energy. A further increase in *V*m was found to increase tensile strengths and ductility. The increasing and then decreasing trend in tensile strength is in contrast to the law of mixture. These unusual behaviors are discussed and explained. Work hardening behavior was analyzed in terms of Holloman analysis.

Keywords Dual phase steel, heat treatment, mechanical properties.

1. Introduction

1-1 Advanced High-Strength Steel (AHSS)

AHSS: A series of high-strength steels containing microstructural phases other than ferrite and pearlite, these other phases include martensite, bainite, and/or retained austenite in quantities sufficient to produce unique mechanical properties. Most AHSS have a multi-phase microstructure [1]. AHSS can be classified according to the microstructure including dual phase (DP), transformation induced plasticity (TRIP) assisted, complex phase (CP) and martensitic (MS) steels.

Fig (1) compares the tensile strength and total elongation of lower strength steels [interstitial free and mild steel], conventional high strength steels (carbon–manganese, bake hardenable and high strength low alloy steels) and AHSS [٢,3].

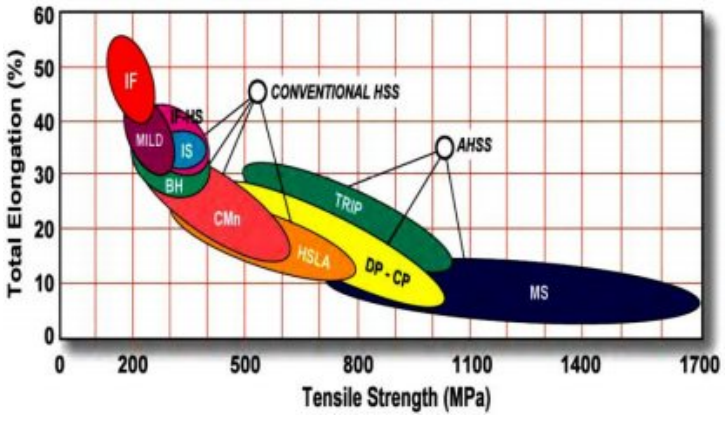

Fig. 1 - Relationship between ultimate tensile strength and total elongation (50.8 mm gauge length) for various types of steel [1].

1-2 Dual Phase Steel

Ferrite–martensite dual phase (DP) steel is one of the most common Advance High Strength Steels (AHSS) which is currently used in automotive industry [4]. Usually ferrite–martensite DP steels are produced by intercritical annealing followed by rapid cooling. During the intercritical annealing small pools of austenite are formed in the ferrite matrix, which subsequently transform into martensite upon rapid cooling. Intercritical heat treatment is the simplest way to enhance low alloys (carbon content less than 0.2%) steels to dual phase microstructure with superior strength–ductility combination [3].

In this combination of two phases, martensite contributes with high strength and ferrite matrix provides good elongation that can produce a good combination of strength and ductility for applications which required good formability. This unique composite microstructure offers other interesting mechanical properties such as continuous yielding, low yield stress to tensile strength ratios and high initial work-hardening rate [2, 5].

1-3 Application of Dual Phase Steel

Fig. 2 shows the use of modern multiphase steels for structural components, taking the example of a new auto body [6]. Honda and BMW as shown in Fig. 3, two car manufacturers that most quickly and warmly welcomed DP grades into their portfolios, have each become known for their forward-thinking use of materials [7]. The wheels in the ULSAB-AVC are made of 1.2 mm DP 350/600 steel and the inner portion is made of 1.8 mm HSLA 490/600, resulting in an optimized, lightweight steel wheel design. The disc is made of 2.1 mm DP 500/800 as shown in Fig. 4. [8].

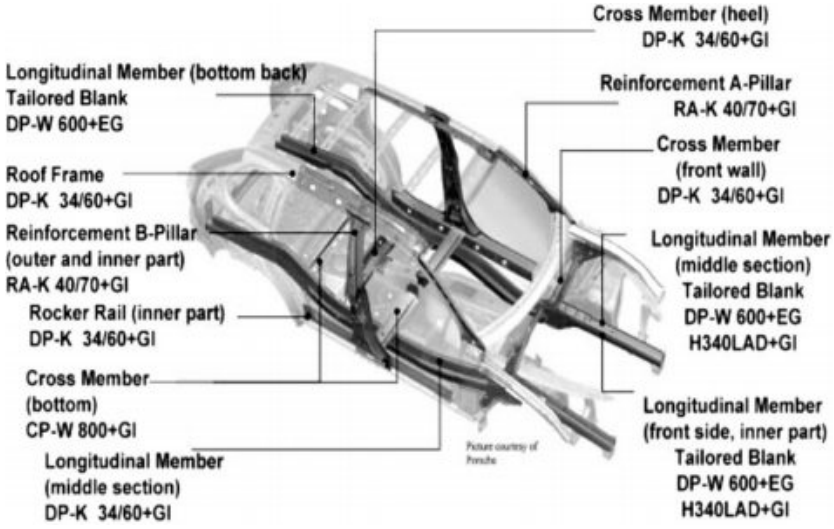

Fig. 2: Application of multiphase steels to the body structures of VW Touareg and Porsche Cayenne [6].

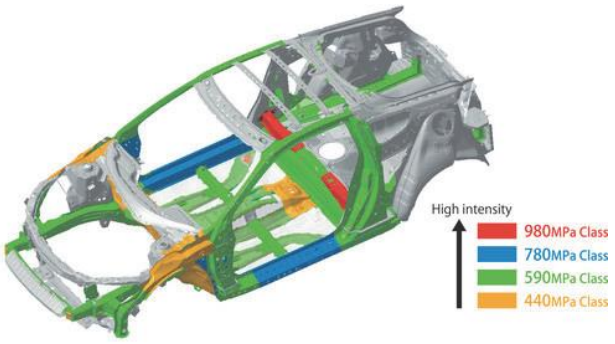

Fig 3: **DP in the 2011 Honda CR-Z [7]**

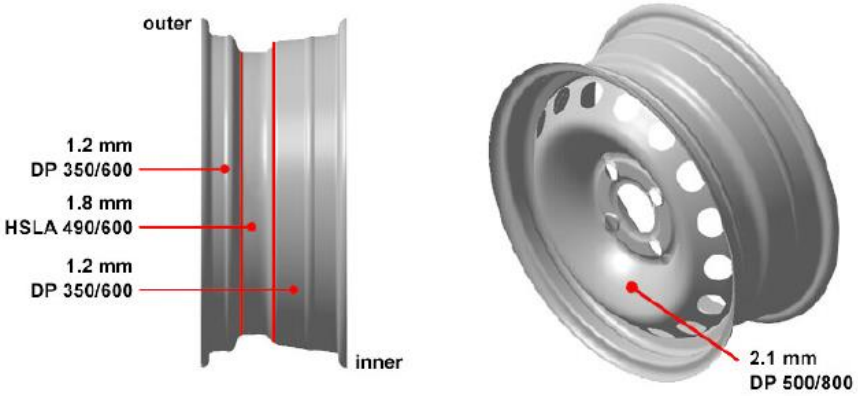

Fig 4: DP steel on wheels [8]

2. Experimental procedure

The steel used in the present investigation was 2-mm in thickness AISI 1005 sheet steel whose chemical composition is given in Table 1. Fig. 5 shows the engineering stress–strain curve and Fig. 6 shows the microstructure of base metal. The microstructure of the base metal sample consists of mainly ferrite with small amount of pearlite.

Table 1: Chemical composition of the investigated steel (weight %).

Element %	C	Mn	P	S	Si	Cr
AISI1005	0.048	0.58	0.03	0.02	0.028	0.02

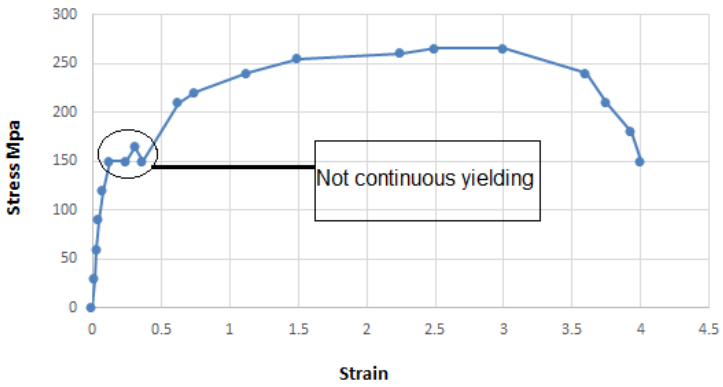

Fig. 5: Engineering stress–strain curve of base metal

Fig. 6: microstructure of base metal sample [80X].

For this study, the AC_1 and AC_3 temperatures were calculated to be 735 and 856 ◦C, respectively by Eqs. (1) And (2) [9].

AC_1 (◦c) = 751−16.3C−27.5Mn−5.5Cu−5.9Ni + 34.9Si +12.7Cr + 3.4Mo (1)

AC_3 (◦c) = 881−206C−15Mn−26.5Cu−20.1Ni−0.7Cr +53.1Si + 41.7V (2)

The heat treatment which is used in this work is shown in Fig. 7. All of the specimens were heated in intercritical temperature range (between AC_1 and AC_3) . All the specimens were held between (5-20) min in (CARBOLITE) furnace as shown in Fig (8) and followed by water quenching (WQ). The heat-treated samples are designated by capital letter, as shown in Fig (7). Metallographic specimens were prepared according to the standard procedure from the base metal and heat-treated samples and etched with 2% nital solution. Microscopic examinations were carried out by an optical microscope.

The tensile test was conducted on base metal and heat-treated specimens with 50mm gage length, 200mm overall length, 20mm width of grip section and 12.5mm width of reduced section using an (QUASAR 25) testing machine as shown in Fig (9) with strain rate of 10mm/min at room temperature in accordance to ASTM E8M [10].

Key parameters obtained from stress–strain curves include yield strength (_YS), ultimate tensile strength (UTS), uniform elongation (UEL), total elongation (TEL) and tensile fracture energy. The amount of energy absorption was digitally calculated by measuring the area under the stress–strain curve up to the final fracture point using the concept of Riemann Sums Eq. (3) [11].

$$\int_0^{Lmax} \mathbf{F}dx = \sum_{n=1}^{N} \mathbf{F}(n).[\mathbf{L}(n) - \mathbf{L}(n-1)] \text{ ----------(3)}$$

Where F is the load, X the displacement, L_{max} the displacement at the peak load, n the sampled data and N the peak load.

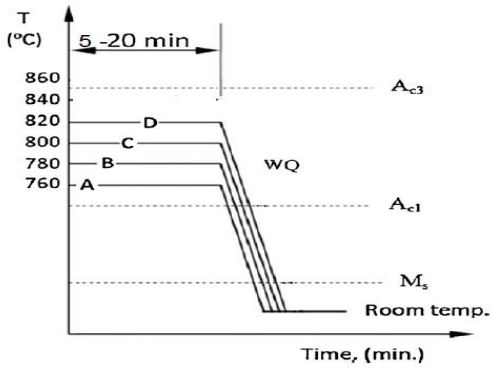

Fig. 7. Schematic illustration of the heat treatment cycle used in this study.

Fig.(8) : Muffle furnace

Fig. (9): QUASAR 25 Testing machine

3. Results and discussion

3.1. Microstructural investigation

The microstructures of the heat-treated samples (A, B and C) are shown in Fig. 10. Increasing Vm is clearly observed in Fig. 10a–c. This complies with lever rule in the ferrite–austenite dual phase region. According to the lever rule, increasing the temperature increases the austenite volume fraction, which then will transform to martensite upon quenching in the water. It worth noticing that by increasing the temperature, Vm increases at higher rate.

Fig. 11 shows variations hardness of the heat-treated samples with increasing heat treatment temperature. Hardness of base metal steel is (134) HV. Hardness of the heat-treated samples

are higher than the hardness of the specimen in the as-received condition. The higher hardness of the dual phase steels due to the presence of the martensite phase.

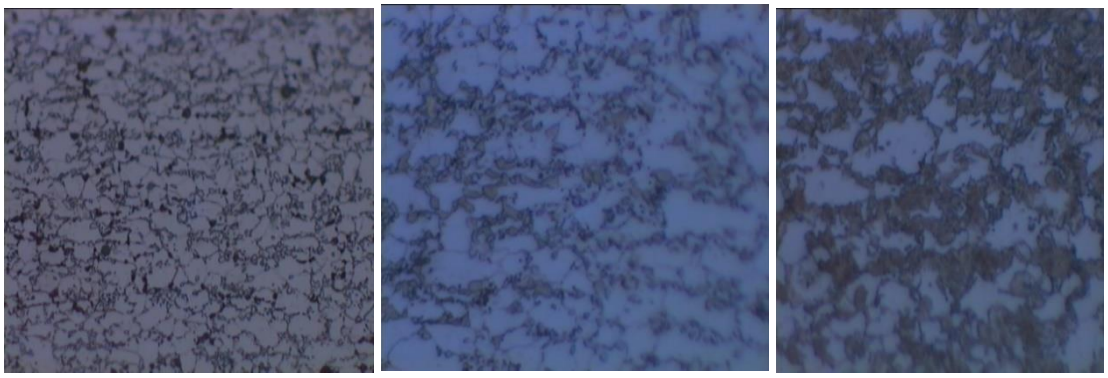

Fig. 10. The microstructures of the heat-treated samples at various intercritical temperatures of (a) 760 ◦C (b) 800 ◦C and (c) 820 ◦C . [80X]

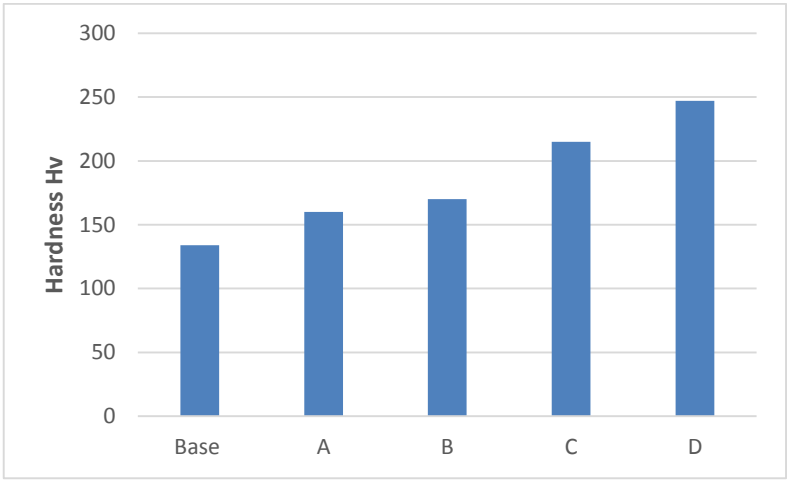

Fig. 11. Hardness for heat-treated samples (A, B, C, D) and Base metal.

3.2. Tensile properties

3.2.1. Continues yielding behavior

The stress–strain curve of the base metal sample has yield point elongation and exhibit well-defined yield point (see Fig. 6). In low carbon steels, this behavior has been attributed to the effect of interstitial solute atoms (carbon), called the Cottrell atmosphere, on locking-in the dislocation. When stress is applied to such steel in a tensile test, it must exceed a certain critical value to unlock the dislocations. The stress necessary to move the dislocations is less than the stress required to unlock them; hence the phenomenon of a sharp yield drop and the appearance of an upper and lower yield point in the tensile stress–strain curve [12].

The yield point has come to be accepted as a general phenomenon, since it has been observed in a number of other metals and alloys. Three factors which control sharp yield point in materials are as follows [13,14]:

1) Low density of mobile dislocation in initial stage of deformation,

2) Rapid dislocation multiplication during plastic deformation and,

3) Low stress dependence of dislocation velocity.

However, this phenomenon is not observed for dual phase steels. As can be seen from Fig. 12 the stress–strain curves of dual phase steels exhibit continuous yielding behavior. The Continues yielding of the ferrite–martensite dual phase has been related to the following [15–16]:

1) Presence of unpinned dislocations which are created in a ferrite matrix via plastic deformation during the austenite to martensite transformation.

2) These unpinned dislocations, located at the ferrite–martensite boundaries are assumed to be mobile in the early stage of plastic deformation.

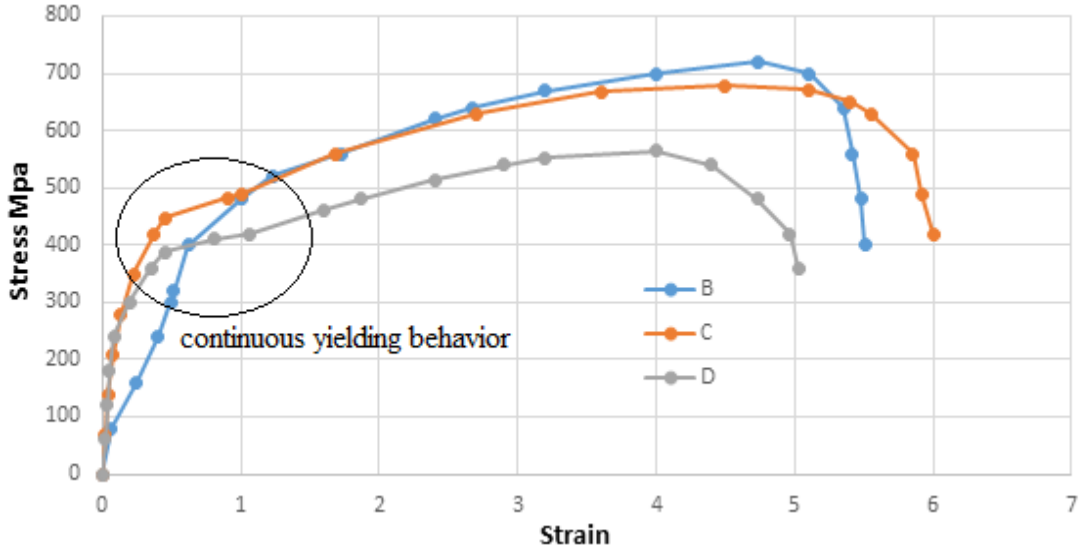

Fig. 12. Engineering stress–strain curves for heat-treated samples (A, D, E).

3.3. Work hardening

The flow behavior of the most metals and alloys can be described by Hollomon Eq. (٤) [17]:

$$\sigma = K\varepsilon^{n} \quad \text{---------- (4)}$$

Where ‘K’ and ‘n’ are constants which are normally called: the strength coefficient and strain hardening exponent, respectively. Drawing the stress–strain data in logarithmic scale and fitting a line to these data, determines the values of these coefficients for the under investigation metal. Stain hardening exponent (n) is the slope of this line and its cross section with ε = 1 (log ε = 0), gives the strength coefficient (K).

Stain hardening exponent (n) is a good indicator for work hardenability of the material.

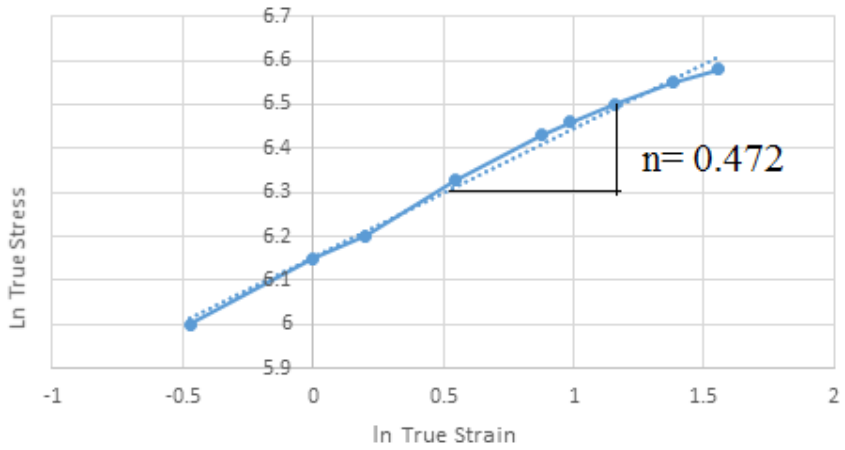

Fig. 13. ln σ –ln ε plot of true stress vs. true strain for investigated steel

3.4 Fracture energy

Fig. 14 shows the effect of temperature of heat treatment on the fracture energy of DP steels. In the automotive industry, the energy absorption capability is an important parameter in vehicle crashworthiness. Variation of fracture energy follows a similar trend for variation of elongation with *V*m. The failure energy increases and maximum failure energy in stage (B). Fracture is understood in terms of the nucleation (either by particle cracking or interfacial decohesion), growth, and coalescence of damage [19]. As the martensite volume fraction increases, its flow stress decreases, resulting in an increase in the potential for martensite to co-deform with the ferrite matrix. In these cases, the nucleation of voids is much more difficult, with the final result being that the fracture strain and fracture energy are increased [19]. It is also interesting to note that 4% volume expansion accompanies the transformation of austenite to martensite. This volume expansion creates a compression stress in the ferrite/martensite interface which impedes the crack growth even if it is nucleated [20]. This can contribute to the increasing energy absorption capability. With further increase in Vm, the matrix structure changes from ferrite to martensite and coherency of the ferrite matrix is also damages by high amount of martensite phase, thus the DP structure becomes brittle and the failure energy is reduced.

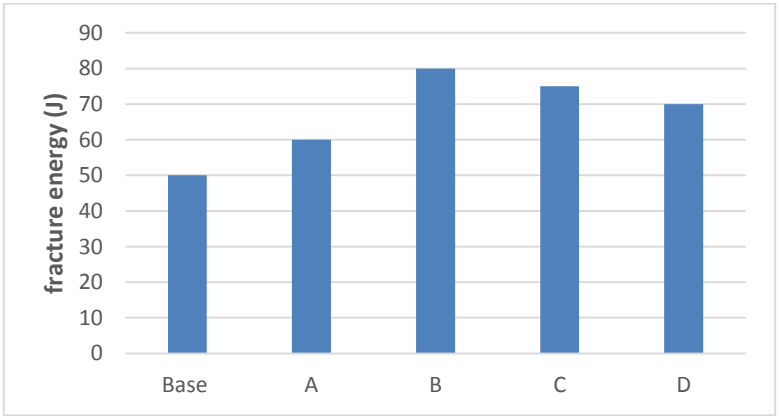

Fig. 14: The variation of the fracture energy with temperature of heat treatment

4. Conclusions

1 – A different samples of dual phase steels containing ferrite and martensite with different volume fractions of martensite (*V*m) was produced by intercritical heat treatment.

2 - It was found that martensite volume fraction increases by increasing the intercritical heat treatment temperature.

3 - Generally, dual phase steels in stage A (780 C, Time 10 S) exhibit the optimum mechanical properties in terms of tensile strength, ductility and fracture energy.

4 - The variations of ultimate tensile strength, ductility and fracture energy with volume fraction of martensite exhibit unusual behavior.

5 - Work hardening behavior was analyzed in terms of Holloman analysis. In this analysis, the work hardening behavior of the samples is single stage.

References

1- American Iron and Steel Institute, "Advanced High Strength Steel (AHSS) Application Guidelines", Washington, Version 4.1, June 2009, Page 1.

2- J. Galán, L. Samek, P. Verleysen, K. Verbeken and Y. Houbaert, "Advanced High Strength Steels for Automotive Industry(·) " rEviSTa DE METalUrGia, Vol 48, No2, P. 118-131, 2012.

3- R. Kuziak, R. Kawalla, S. Waengler, "Advanced High Strength Steels for Automotive Industry" Archives of Civil And Mechanical Engineering, Vol VIII, No. 2, p. 103-117, 2008.

4- X. Sun, E. Stephens and M. Khaleel," Effects of Fusion Zone Size on Failure Modes and Performance of Advanced High Strength Steel Spot Welds ", SAE, paper series 2006-01-0531.

5- M. Delince, Y. Brechet, JD. Embury, MGD. Geers, PJ. Jacques, T. Pardoen, Separation of size-dependent strengthening contributions in fine-grained Dual Phase steels by nanoindentatio, Acta. Mater. 55 (2007) 2337-2350.

6- H. Hofmann, D. Mattissen, T. W. Schaumann, "Advanced cold rolled steels for automotive applications", Mat.-wiss. u. Werkstofftech, Vol 37, No. 9, P. 716-723, 2006.

7- Ultra Light Steel Auto Body Consortium, overview report, Wiley, January 2002

8- The Evolving Use of Advanced High-Strength Steels for Automotive Applications, Steel Market Development Institute 2000 Town Center, Suite 320 Southfield, Michigan

9- F. Hayat, "Comparing Properties of Adhesive Bonding Resistance Spot Welding and Adhesive Weld Bonding of Coated and Uncoated DP 600 Steel ", Journal Of Iron And Steel. Research, International. Vol 18, No 9: P. 70-78, 2011.

10- Standard Methods of Tension Testing of Metallic Materials, E 8. Annual book of ASTM standards, vol. 03.01. ASTM, Philadelphia; 2004. p. 130–150.

11- H. Zhang and J. Senkara: "Resistance Welding: Fundamentals and Applications", CRC Group, London, New York, 2006.

12- M.A. Meyers, K.K. Chawla,W.F. Hosford, Mechanical Behavior of Materials, seconded., Cambridge University Press, 2008.

13- G.E. Dieter, Mechanical Metallurgy, second ed., Published by McGraw-Hill, 1976.

14- R.W. Hertzberg, Deformation and Fracture Mechanics of Engineering Materials, John Wiley & Sons, 1996.

15- M.A. Maleque, Y.M. Poon, H.H. Masjuki, The effect of intercritical heat treatment on the mechanical properties of AISI 3115 steel, Journal of Materials Processing Technology, Volumes 153-154, 10 November 2004, Pages 482-487.

16- Jinxing Jiang, Huibin Wu, Jinming Liang, Di Tang, Microstructural characterization and impact toughness of a jackup rig rack steel treated by intercritical heat treatment. Materials Science and Engineering: A, Volume 587, 10 December 2013, Pages 359-364

17- J.H. Hollomon, Trans. AIME 162 (1945) 268.

18- Mohammad Reza Akbarpour, A. Ekrami, Effect of temperature on flow and work hardening behavior of high bainite dual phase (HBDP) steels, Materials Science and Engineering: A, Volume 475, Issues 1–2, 25 February 2008, Pages 293-298

19- G. Rosenberg, I. Sinaiová, Ľ. Juhar Effect of microstructure on mechanical properties of dual phase steels in the presence of stress concentrators. Materials Science and Engineering: A, Volume582, 10 October 2013, Pages 347-358

20- H. Saghafian, Sh. KheirandishCorrelating microstructural features with wear resistance of dual phase steel Materials Letters, Volume 61, Issues 14–15, June 2007, Pages 3059-3063